

Changes in the electronic structure of highly compressed iron revealed by X-ray fluorescence lines and absorption edges



S.B. Hansen*, E.C. Harding, P.F. Knapp, M.R. Gomez, T. Nagayama, J.E. Bailey

Sandia National Laboratories, Albuquerque, New Mexico 87185, USA

ARTICLE INFO

Article History:

Received 30 June 2017

Accepted 7 July 2017

Available online 10 July 2017

ABSTRACT

We present high-resolution spectroscopic data from iron impurities in beryllium liners driven by Sandia's Z machine to temperatures near 10 eV and electron densities near $2 \times 10^{24} \text{ cm}^{-3}$, conditions independently diagnosed from the transmission depth and shape of the iron K-edge. A 12-eV redshift is observed in the Fe $K\beta$ fluorescence line along with few-eV shifts in the Fe $K\alpha$ lines and Fe K-shell absorption edge. While the measured edge shift disagrees with several common models of ionization potential depression, both line and edge shifts are in good agreement with the predictions of a self-consistent model based on density functional theory.

© 2017 Elsevier B.V. All rights reserved.

Introduction

Investigations into the structure and characteristics of warm dense matter (WDM) have become active in recent years due to its importance for astrophysics and inertial confinement fusion. WDM is fundamentally challenging to model since it lies at the intersection of condensed matter and plasma physics where thermal, degeneracy, and strong coupling effects all contribute to the material properties. At high densities, models predict changes in electronic structure that lead to phenomena such as ionization potential depression (IPD), pressure ionization, metal-non-metal transitions, and density-driven line shifts (also called plasma polarization shifts). But while advances in experimental drivers have enabled the creation of increasingly large and uniform samples suitable for benchmark studies of extreme material conditions, diagnosing these dense-plasma phenomena in WDM remains difficult due to its high opacity and limited self-emission.

Early experimental work on IPD used backlighting spectroscopy to measure the aluminum K-edge in shock-compressed aluminum [1] and showed reasonable agreement with existing models. At the conditions accessible on modern facilities, however, discrepancies between experiment and theory have been observed. In 2012, fluorescence x-ray emission from multiply-ionized solid-density aluminum [2] indicated ionization levels higher than predicted by standard Stewart–Pyatt IPD theory [3]. These measurements stimulated renewed interest in some older IPD models such as Ecker–Kroll [4] as well as new work on the fundamental origin of dense plasma effects on electronic structure [5–7]. They also spurred the development of new techniques to measure IPD from plasmas in a

variety of coupling and degeneracy regimes, including x-ray scattering from warm, highly compressed carbon [8,9] and thermal self-emission spectroscopy of high- n lines from hot compressed aluminum [10]. In general, none of these data are fully consistent with any of the ad-hoc IPD models currently implemented in the non-equilibrium spectroscopic models often used to diagnose high-energy-density plasmas. Recently, simulations of x-ray-driven fluorescence emission based on density-functional theory (DFT) with imposed core-hole excitations [7] have been shown to be consistent with data from a variety of materials and mixtures [11], however it is not yet clear how best to combine the self-consistent electronic structure from a DFT model with non-equilibrium models that generate detailed emission, scattering, or fluorescence spectra suitable for direct comparison with experimental measurements. And it remains unclear why the Stewart–Pyatt IPD model, which in its high-density limit approaches a DFT-based ion-sphere model [12], fails to describe many of the recent observations from dense plasmas.

Like IPD effects, plasma polarization shifts originate from free-electron screening and are expected to be most pronounced at high densities. To date, however, observations of this shift in X-ray lines [13–15] have been limited to thermal emission from highly charged ions, where satellites, opacity, line broadening, Doppler, and instrumental effects cannot all be definitively excluded as the origin of the shifts.

Here we present high-resolution fluorescence and edge absorption spectra from the dense material shell surrounding an inertially confined fusion plasma, bringing new data to bear on models of both IPD and plasma polarization. The combination of this platform (dense, degenerate material backlit by a hot plasma) and measurement technique (high resolution fluorescence and absorption spectroscopy) offers a new test of dense plasma theory and its implementation in diagnostic models. The experimental spectrum

* Corresponding author.

E-mail address: sbhans@sandia.gov (S.B. Hansen).

includes in-situ energy fiducials and its interpretation is unmediated by complex models of x-ray scattering, non-equilibrium photoionization and fluorescence, or density-dependent line shapes. The iron transmission above the K edge is used to infer the plasma density while the electron temperature is determined from fits to the spectral shape of the edge itself. This enables model validation based on the measured energy shifts of the iron K-edge and fluorescence lines. We find good agreement with shifts predicted by a DFT-based average-atom model [16,17] and disagreement with several ad-hoc IPD models [3,4,12].

Experimental data and analysis

The measurements were made on Sandia's Z facility, where approximately 20 MA of current drives the implosion of a solid beryllium liner filled with deuterium gas. This is the Magnetized Liner Inertial fusion (MagLIF) platform [18–22]. The cylindrical liners have an initial outer radius of 2.79 mm and inner radius of 2.325 mm, for an initial areal density of 0.086 g/cm^2 . They implode with peak velocities of $\sim 70 \text{ }\mu\text{m/ns}$, compressing the pre-heated and pre-magnetized fuel into a hot core. At stagnation, the $\sim 8 \text{ mm}$ tall core has fuel densities of $\sim 0.3 \text{ g/cm}^3$ ($n_e \sim 10^{23} \text{ cm}^{-3}$), burn-averaged temperatures of $T_e \sim T_{\text{ion}} \sim 2.5 \text{ keV}$, and radius of $\sim 50 \text{ }\mu\text{m}$, producing $\sim 2 \times 10^{12}$ D-D neutrons and bright continuum X-rays [19,22].

As X-rays from the hot core pass through the cold, compressed beryllium liner, they photoionize K-shell electrons in Fe and Ni impurities present in the liner, producing cold $K\alpha$ and $K\beta$ fluorescence emission as illustrated in Fig. 1. The emitted X-ray spectra are measured by the XRS3 [23], a highly resolving, spherically focusing, and axially imaging spectrometer with both spatial ($200 \text{ }\mu\text{m}$) and spectral ($E/\Delta E > 3500$) resolution. The energy dispersion is calibrated to an accuracy of $\pm 1.2 \text{ eV}$ over a 6–8 keV spectral range, anchored to thermal Fe and Ni $\text{He}\alpha$ emission lines at 6.701 and 7.806 keV that arise from liner material mixed into the hot core. An imaged spectrum is given in Fig. 1(c) showing continuum and thermal line emission from the hot core along with fluorescence emission from the Fe and Ni impurities in the cold, compressed liner. High spatial correlation between the continuum and fluorescence-line intensities indicates that the fluorescence is produced by photoionization from the hot stagnation plasma rather than electron beams potentially generated in an unstable implosion. The observed

K-shell edge of Fe is due to continuum x-rays directly absorbed by the liner along the instrument line of sight.

Spectral lineouts from two experiments are given in Fig. 2, showing that increasing the Fe impurity concentration by 65% leads to corresponding increases in fluorescence emission and K-edge absorption. With the Fe concentration known to $\pm 5\%$, the cold liner opacity can be used to constrain the liner areal density (ρR) to within $\pm 15\%$ by fitting the change in transmission across the Fe K-edge. While the exact energy and shape of the K edge can be affected by changes in the valence M-shell electron structure, its strength depends on deeply bound K-shell electrons that are depopulated only at keV-scale temperatures. The K-edge diagnostic is illustrated for a recent experiment (shot z2979) by the dashed red line in Fig. 2. Here, the K-edge absorption indicates $\rho R = 0.75 \text{ g/cm}^2$ and an edge shift of $+5 \text{ eV}$. The solid red line shows the same edge softened by a 10 eV temperature whose shape is determined by the temperature-dependent Fermi electron distribution function: $f(\epsilon) = \{1 + \exp[(\epsilon - \mu)/T_e]\}^{-1}$ with μ the temperature-dependent chemical potential. In highly degenerate matter, $\mu \sim \epsilon_{\text{Fermi}} \sim 1.7 \text{ eV} \times (n_e/10^{22} \text{ cm}^{-3})^{2/3}$. For WDM with $T_e < \epsilon_{\text{Fermi}}/4$, the K-edge shape provides a direct temperature estimate [24]. The spectrum from z2977, with only 110 ppm Fe, has a similar areal density and temperature with decreased absorption due to its smaller Fe concentration. While axial variations of $\pm 20\%$ in both ρR and T_e are present in both experiments, both have average liner ρR values near 0.8 g/cm^2 , which is consistent with the 0.9 g/cm^2 values independently determined from filtered diodes [19,22]. Assuming uniform compression, a final inner radius of $50 \text{ }\mu\text{m}$, and no loss or axial redistribution of liner mass, the mass density can be determined directly from the areal density: $\rho R = 0.75 \text{ g/cm}^2 \pm 10\%$ implies approximately eightfold compression of the initial liner at stagnation, corresponding to a mass density of $15 \pm 4 \text{ g/cm}^3$ and electron density near $2 \times 10^{24} \text{ cm}^{-3}$ for Be with ionization $Z^* \sim 2$. The corresponding $\epsilon_{\text{Fermi}} \sim 60 \text{ eV}$ confirms the applicability of the temperature diagnostic.

Simple models of density-dependent line shifts [25,26] predict that $n_e \sim 2 \times 10^{24} \text{ cm}^{-3}$ is sufficient to cause plasma polarization shifts on the order of several eV, and indeed redshifts of 1–2 eV in $K\alpha$ and 12 eV in Fe $K\beta$ are observed in the measured fluorescence lines. To definitively isolate the effects of free-electron screening in the $K\alpha$ and $K\beta$ fluorescence lines, we must consider potential contributions to line shifts from at least three other sources: 1) instrumental uncertainties, 2) motional Doppler shifts, and 3) bound-electron screening due to temperature- and density-dependent ionization.

Instrumental effects can be ruled out as the source of the 12 eV $K\beta$ shift given the $\pm 1.2 \text{ eV}$ dispersion accuracy, which is confirmed by thermal emission lines on both sides of $K\beta$. These thermal lines provide in-situ energy fiducials since they are emitted from the high-temperature and low-density core and are not expected to be shifted. (Note that while the thermal Fe and Ni emission arises from liner mix, Co was introduced as a fuel-only tracer in z2977.) Motional Doppler shifts can also be ruled out as the source of the $K\beta$ shift, since they are only $\sim 1.6 \text{ eV}$ at the peak implosion velocity and would be similar for both $K\alpha$ and $K\beta$.

To assess the effects of bound-electron screening, we compare in Fig. 3 the shifts in iron $K\alpha$ and $K\beta$ fluorescence lines under progressive ionization of 3d electrons from three different models. The most accurate of these models for isolated ions is FAC [27], a relativistic multiconfiguration Dirac-Fock atomic structure code with extensive configuration interaction. Although the FAC atomic data is based on isolated-ion calculations, its absolute predictions for the $K\alpha$, $K\beta$, and even $K\beta'$ satellite energies are within 2 eV of ambient iron reference data. The FAC points in Fig. 3 include error bars representing the typical spread in transition energies arising from multiple fine-structure transitions. A second model, LIMBO [28], is a DFT-based relativistic self-consistent field code that provides orbital energies for isolated

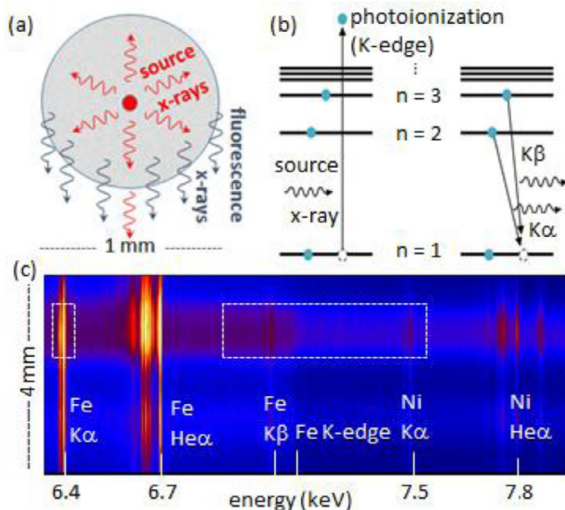


Fig. 1. (a) Top-down schematic of source plasma illustrating fluorescence line production and continuum absorption along the spectrometer line of sight. (b) Diagram illustrating electronic transitions of photoionization and fluorescence. (c) Axially-resolved spectrum with dashed boxes indicating lineouts used for liner diagnostics.

Download English Version:

<https://daneshyari.com/en/article/5486871>

Download Persian Version:

<https://daneshyari.com/article/5486871>

[Daneshyari.com](https://daneshyari.com)